Identification of Photocatalytic Degradation Products of Diazinon in TiO$_2$ Aqueous Suspensions Using GC/MS/MS and LC/MS with Quadrupole Time-of-Flight Mass Spectrometry

Vasilis N. Kouloumbos and Despina F. Tsipi
General Chemical State Laboratory, Athens, Greece

Anastasia E. Hiskia
Institute of Physical Chemistry NCSR "Demokritos", Athens, Greece

Dejan Nikolic and Richard B. van Breemen
Department of Medicinal and Pharmacognosy, University of Illinois College of Pharmacy, Chicago, Illinois, USA

The photocatalytic degradation of the organophosphorus insecticide diazinon in aqueous suspensions has been studied by using titanium dioxide as a photocatalyst. The degradation of the insecticide was a fast process and included the formation of several intermediates that were identified using GC/ion-trap mass spectrometry with EI or CI in positive and negative ionization mode and HPLC/electrospray-QqTOF mass spectrometry. Since primarily hydroxy derivatives were identified in these aqueous suspensions, the mechanism of degradation was probably based on hydroxyl radical attack. The initial oxidative pathways of the degradation of diazinon involved the substitution of sulfur by oxygen on the P=S bond, cleavage of the pyrimidine ester bond, and oxidation of the isopropyl group. Exact mass measurements of the derivatives allowed the elemental formula of the molecules to be determined confidently. Similarities to the metabolic pathways occurring in living organisms were observed.   (J Am Soc Mass Spectrom 2003, 14, 803–817) © 2003 American Society for Mass Spectrometry

Diazinon [O,O-diethyl O-(2-isopropyl-6-methylpyrimidin-4-yl) thiophosphate] is an organophosphorus insecticide with widespread agricultural and non-agricultural uses. The primary environmental concerns associated with its use are bird kills, contamination of surface water, and impacts on aquatic species. Diazinon and its metabolites have been encountered during monitoring studies in various aquatic systems all over the world [1–3]. Additionally, high diazinon residues have been found in urban waterways and effluents from sewage treatment plants [4, 5].

Toxic effects of diazinon are due to the inhibition of acetylcholinesterase. Metabolic studies in animals have shown that the main route of metabolism is oxidation, and several metabolites with higher acetylcholinesterase inhibition activity have been identified [6]. Because

of the great risk that it poses to human health and the environment, diazinon use has been reviewed by many European environmental agencies in the past decade. Recently the U.S. Environmental Protection Agency announced a three-year phase-out of diazinon for indoor use, because it is one of the leading causes of acute insecticide poisoning of humans and wildlife [7].

In the environment, diazinon appears to be mobile and persistent enough to significantly impact water resources. The abiotic environmental fate of diazinon has been well studied previously; it is stable at neutral waters, while it is rapidly hydrolyzed at acidic pH [8]. Hydrolysis products have been identified as 2-isopropyl-6-methyl-pyrimidin-4-ol (IMP) and diethyl thiophosphate [9]. Diazinon is slowly photodegraded in distilled water under sunlight, while in natural waters the process is significantly faster [10, 11]. 2-Isopropyl-6-methylpyrimidin-4-ol has been identified as the main photoproduct [8]. Photolysis studies of diazinon in soil aqueous suspensions under UV light have shown that the main transformation products are its oxygen analogue,

diethyl 2-isopropyl-6-methylpyrimidin-4-yl phosphate (diazoxon), its isomer O,O-diethyl S-(2-isopropyl-6-methylpyrimidin-4-yl) thiophosphate) (isodiazinon), and O,O-diethyl O-[2-(1-hydroxy-1-methylethyl)-6-methylpyrimidin-4-yl] thiophosphate (hydroxydiazinon) [9]. Because diazinon transformation products are more polar than the parent compound, they may be consequently more water soluble, more mobile, and have a greater potential to leach from soil. Therefore, these compounds would probably be found in surface and ground water at higher concentrations than the parent compound.

Solar photocatalytic water treatment with irradiated semiconductors has been proposed as an effective and environmentally attractive technique for degradation and final mineralization of organic pollutants into CO_2 and inorganic anions [12, 13]. TiO_2 photocatalytic decomposition has been studied extensively for many organic compounds, including various classes of pesticides [14–17]. The initial step of the heterogeneous photocatalytic process is the excitation of TiO_2 with light at near-visible UV to produce conduction band electrons (e^-_{cb}) and valence band holes (h^+_{vb}). The redox potential of the photogenerated holes is able to oxidize organic molecules adsorbed on the TiO_2 surface by combination of direct oxidation reactions and production of oxidizing species after reaction with water, such as hydroxyl radicals. Recombination of the electron-hole pairs provides a competitive route for the catalytic process, so that the presence of oxidizing species, commonly dilute O_2, is essential for the removal of the generated electrons [18]. Repeated oxidation of the organic intermediates leads to the mineralization of the compounds.

The photocatalytic degradation of diazinon in aqueous suspensions by using TiO_2 as a photocatalyst has been shown to be effective leading to the production of CO_2 and inorganic ions. Although parent compound degradation is achieved usually in a few minutes, PO_4^{3-}, NH_4^+, and NO_3^- production and total organic carbon (TOC) reduction follow much slower rates [19–23]. At present, no studies on diazinon photocatalysis intermediates have been reported, and a detailed study of the photocatalytic degradation process might provide useful information for the optimization of the overall photocatalytic system. Since the formation of highly toxic reaction intermediates is possible, identification of the degradation products is essential. Furthermore, the elucidation of the mechanism of the photocatalysis might be useful for the prediction of degradation of other substrates using the same catalyst [24]. Since photocatalytic degradation has been suggested to be similar to biological processes, insights might be obtained from these studies regarding metabolic transformation of diazinon in living organisms [25].

The purpose of this study was to analyze the photocatalytic degradation products of diazinon using GC/ion-trap mass spectrometry and HPLC/quadrupole-time-of flight (QqTOF) mass spectrometry. For identification, structural data were obtained on an ion trap mass spectrometer following electron impact ionization (EI), positive ion chemical ionization (CI) and negative ion chemical ionization (NCI). These data were complemented with exact mass measurements on both precursor and fragment ions obtained using a QqTOF mass spectrometer. A degradation pathway for diazinon is proposed based on the identified intermediates and also compared with the metabolic pathways in living organisms.

Experimental

Chemicals and Reagents

Diazinon (94.0%) was purchased from Dr. Ehrenstorfer (Augsburg, Germany). Diazoxon (>90%), sulfotep and 2-isopropyl-6-methylpyrimidin-4-ol (IMP) (99%) were obtained from Chem Service (West Chester, PA). TiO_2 P25 (mainly in anatase form) was obtained from Degussa (Dusseldorf, Germany). Dichloromethane and acetone (Labscan, Dublin, Ireland) were pestiscan grade. HPLC-grade water (Labscan) was used for the preparation of the catalytic suspensions. Anhydrous sodium sulphate was purchased from Riedel-de Haen (Seelze-Hannover, Germany), sodium carbonate from Fluka (Buchs, Switzerland) and perchloric acid from Merck (Darmstadt, Germany).

Irradiation Experiments

Irradiations were performed in Pyrex cylindrical cells (total volume, ca. 50 mL, diameter, 4.5 cm) using four Blacklight-Blue F15W/T8/BLB lamps (Sylvania, Danvers, MA) emitting mainly at 300–400 nm. The distance between the irradiated solutions and the lamps was 17 cm. The irradiations were carried out on 5 mL pesticide suspensions containing 20 mg L^{-1} diazinon and 500 mg L^{-1} TiO_2. Diazoxon (20 mg L^{-1}) in TiO_2 aqueous suspensions was also irradiated under the same conditions. During irradiation, the samples were magnetically stirred. All experiments were carried out at room temperature and pH 6.

Sample Extraction

The irradiated aqueous solutions were extracted two times using dichloromethane (10 mL). The combined dichloromethane phases were passed through 5 g of anhydrous sodium sulphate, rotary evaporated to ~1 mL and then diluted to 5 mL with acetone. The solvent was concentrated once more in a rotary evaporator to ~1 mL and evaporated under a gentle stream of nitrogen to dryness. The residue was redissolved in 200 μL of acetone for GC/MS or methanol for LC/MS analysis. 100 μL of this concentrated extract was diluted to 1 mL with acetone for GC/MS analysis of diazinon and diazoxon.

Carbon Dioxide Evolution

Evolution of carbon dioxide produced during irradiation of diazinon in TiO_2 aqueous suspensions was followed by head-space gas chromatographic analysis of the gas phase of Pyrex cells by GC/MS in EI mode at 70 eV electron energy, monitored from m/z 10–360. The column used was an AT-5MS (Alltech, Deerfield, IL), fused silica capillary column (30 m, 0.25 mm i.d., ft 0.25 μm). The oven temperature program was 1.2 min at 40 °C, 4.2 °C/min to 50 °C, 16.7 °C/min to 80 °C (1.2 min). The injector temperature was 210 °C, and the transfer line temperature was 275 °C. The samples were oxygenated before irradiation, and 100 μL from the gas phase was injected splitless. Extracted chromatograms of the ion of m/z 44 were used for the detection and quantitation of the CO_2 peak. Calibration curve was obtained using $Na_2CO_3/(HClO_4$ 0.1 M) standard solutions. Blank CO_2 values produced during irradiation of TiO_2 suspensions in the absence of diazinon were substracted from the total CO_2 produced.

Analytical Procedures

HPLC/DAD analysis. HPLC analyses were carried out using a Waters (Milford, MA) Model TM 600 gradient pump, 966 DAD and a 717 autosampler. Data were processed using Waters Millenium software (version 2.10). The analytical column was a Waters C_{18} Nova-Pak, 4.6 × 250 mm, the mobile phase was isocratic acetonitrile/water, 70:30 (vol/vol), at a flow rate of 1 mL/min, and the eluate was monitored at 254 nm. The irradiated solutions were filtered through 0.45 μm Millipore (Bedford, MA) Millex-LCR filters before HPLC analysis. The injection volume was 20 μL.

GC/MS and GC/MS^n analysis. A ThermoFinnigan (Austin, TX) GCQ gas chromatograph-ion trap mass spectrometer with an AS 2000 autosampler and Xcalibur (version 1.1) software for data acquisition and processing was used for GC/MS and GC/MS^n analyses. The gas chromatographic analysis was performed with an Alltech AT-5MS fused silica capillary column (1. = 30 m, i.d. = 0.25 mm, f.t. = 0.25 μm). The helium carrier gas velocity was 30 cm/s, the injector temperature was 210 °C, and the transfer line temperature was set at 275 °C. The oven program was 1 min at 60 °C , 20 °C/min to 80 °C, 5 °C/min to 196 °C, and 20 °C/min to 270 °C (10 min). Ions were formed for mass spectrometric detection using either positive ion electron impact ionization (EI), positive ion chemical ionization (CI) or negative ion chemical ionization (NCI). During CI and NCI, methane was used at the reagent gas at a manifold pressure of 70 mTorr. EI mass spectra database searches were carried out using the Wiley (New York, NY) Registry of Mass Spectral Data, 6th edition, and the NIST Mass Spectral Search Program version 1.6d, Search Type: Identity, Normal. The concentrated extracts (2 μL aliquots) were injected splitless. The mass
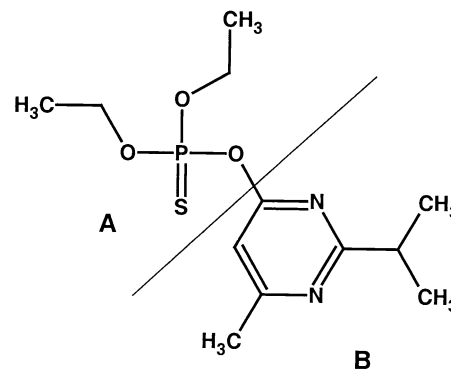

Figure 1. Molecular structure of the insecticide diazinon. Thiophosphoric moiety (a) and pyrimidine group (b) are shown.

spectrometer detector was set to be off at the time of diazinon elution, to avoid filament damage during sample analysis. Diluted extracts were analyzed for monitoring the diazinon and diazoxon and the mass spectrometer detector was not set to be of during sample analysis.

QqTOF LC/ESI-MS and LC/ESI-MS/MS analysis. Positive ion electrospray LC/MS analysis was carried out using a Micromass (Manchester, UK) Q-TOF-2 hybrid quadrupole-time-of-flight mass spectrometer. Degradation products of diazinon were separated using an YMC (Wilmington, NC) C_{18} AQ column, 2.0 × 250 mm, with isocratic acetonitrile/water (65:35, vol/vol) as the mobile phase. The flow rate was 0.2 mL/min. High-resolution exact mass measurements were carried out on-line by adding reserpine post-column as a lock mass. Data were acquired at 10,000 FWHM resolution. Calibration was carried out using polyethylene glycol shortly before the sample analysis. To avoid dead-time distortion, the concentration of the lock mass was adjusted to provide approximately 140 counts/s as monitored on a real-time display. Exact mass measurements of fragment ions were carried out using the precursor ion as the lock mass. Product ion mass spectra were acquired at a collision energy of 15 or 25 eV (for follow-up measurements) using argon as the collision gas.

Results and Discussion

Photocatalytic Degradation

The photocatalytic degradation of diazinon (see structure in Figure 1) over time in pure water in the presence of TiO_2 was monitored by using HPLC/DAD. The kinetics of diazinon disappearance in the presence or absence of TiO_2 is shown in Figure 2a. During irradiation in the presence of TiO_2 diazinon degraded rapidly and disappeared completely within 30 min. In contrast, irradiation of diazinon in the absence of TiO_2 produced minimal photolytic degradation. Control experiments performed in the dark indicated that hydrolysis and
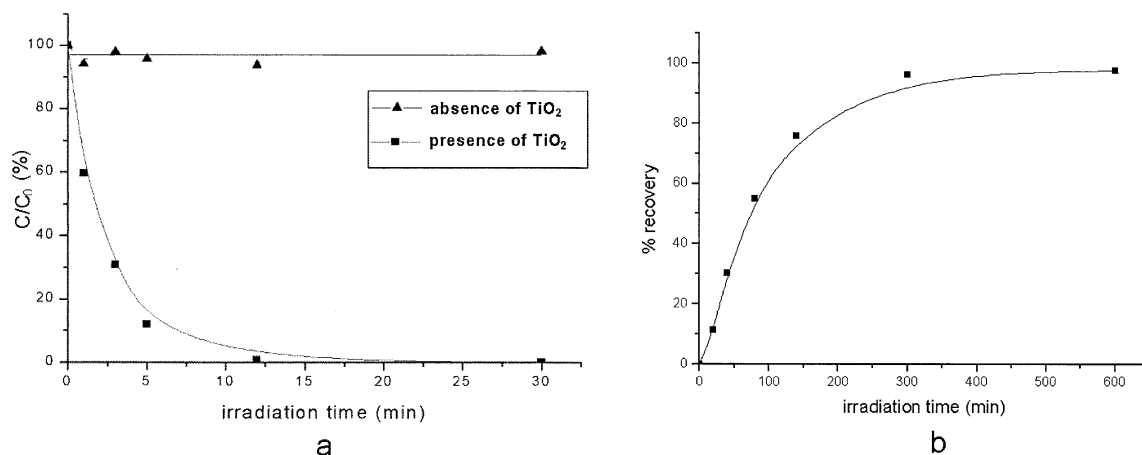
Figure 2. (a) Photodegradation of diazinon aqueous solution (C = 20 mg L^{-1}) in the absence and in the presence of TiO$_2$ (C = 500 mg L^{-1}) (b) Formation of CO$_2$ after photocatalytic oxidation of diazinon in the presence of TiO$_2$.

adsorption of diazinon on TiO$_2$ particles did not affect its concentration during these experiments.

The evolution of CO$_2$ was monitored by using headspace GC/MS, and these measurements established that only 10% of the carbons in the diazinon molecule were totally oxidized by the time the intact pesticide was no longer detected (Figure 2b). Total mineralization of diazinon occurred after 5 h of irradiation. Even though mineralization of diazinon also leads to the production of inorganic ions, this process will not be discussed.

Organic Intermediates Monitoring

When the semiconductor TiO$_2$ is irradiated with light of wavelength $\lambda \leq 390$ nm, valence band holes (h$^+_{vb}$) and conduction band electrons (e$^-_{cb}$) are photogenerated (eq 1). OH radicals generated through water oxidation by photo-generated valence band holes according to eq 2, are known to be the most oxidizing species [26].

$$TiO_2 + h\nu \rightarrow h^+_{vb} + e^-_{cb} \tag{1}$$

$$h^+_{vb} + H_2O \rightarrow OH^\bullet + H^+ \tag{2}$$

OH radicals react rapidly and non-selectively with organic molecules leading to the production of numerous oxidation intermediates and final mineralization products. In the presence of air, other species might contribute to the oxidation of the organic molecules, such as H$_2$O$_2$ or even superoxide radicals, which are produced by oxygen reduction through photogenerated conduction band electrons (eqs 3, 4).

$$2H^+ + 2e^-_{cb} + O_2 \rightarrow H_2O_2 \tag{3}$$

$$e^-_{cb} + O_2 \rightarrow O_2^{\bullet-} \tag{4}$$
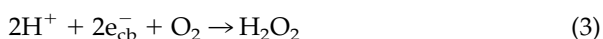
The nature of diazinon photocatalytic degradation

products was studied using GC/MS and LC/MS. A reaction pathway is proposed including the identified intermediates.

GC/MS. The concentrated aqueous suspension extracts were analyzed by using GC/MS. After 3 min irradiation, several degradation products not present in a blank control were detected during GC/MS with positive ion EI (see Figure 3). Most of the degradation products eluted after diazinon (RT 26.6 min). The mass spectrometer detector was set to be off at the time of diazinon elution. Spectra for diazinon and Compound (**2**) were obtained after GC/MS analysis of diluted samples, where the detector was not set be off. The following general approach was followed for the identification of each degradation product. First, the molecular mass of each of the unknown compounds was determined using positive ion CI mass spectrometry through the abundant protonated molecule and the characteristic [M + C$_2$H$_5$]$^+$ and [M + C$_3$H$_5$]$^+$ adducts, and then structural data were obtained from the EI fragmentation patterns and library searching. In addition, MS^2 and MS^3 provided information regarding the identities of the fragment ions. NCI mass spectra gave useful information regarding the presence of particular substructures containing electronegative atoms. For organophosphate compounds NCI mode is generally more sensitive than either positive ion CI or EI [27]. The commercial standards were analyzed using GC/MS under the same conditions as the suspension extracts. The retention times and mass spectra of standards and unknown degradation products were compared.

MS/MS analysis of the fragment ions of diazinon (Mr 304) gave information regarding the structures of the characteristic ions of the pyrimidine moiety. The base peak at m/z 179 and the ions of m/z 137 and 152 in the EI mass spectrum of diazinon (Figure 4a) corresponded to the structure of the ethyl ether of pyrimidinol and the pyrimidine structures shown in Figure 4b.
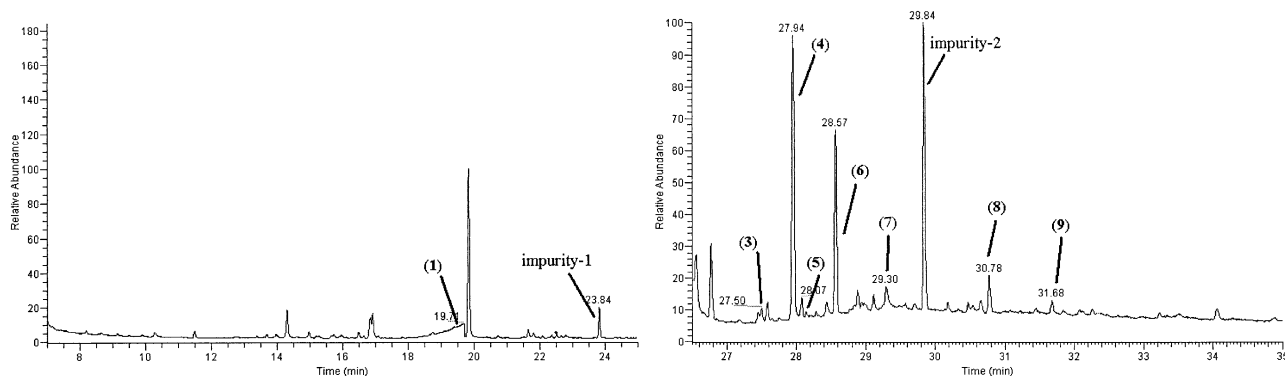
Figure 3. GC/MS chromatogram of a diazinon aqueous catalytic suspension concentrated extract after 3 min of irradiation. Nine oxidation intermediates and two standard impurities were detected. The detector filament was set to be off at the time of diazinon elution (RT 26.6 min). Spectra for diazinon and Compound (**2**) were obtained after GC/MS analysis of diluted samples, where the detector was not set be off.

These ion structures have been reported in a previous study [28]. The structure of the ion at m/z 135 also corresponded to the pyrimidine group. MS/MS analysis of the ion of m/z 135 resulted in a product ion of m/z 93 corresponding to the loss of a C_3H_6 group. Subsequently, one molecule of HCN (originating from the pyrimidine group) was eliminated resulting in the ion of m/z 66 followed by an additional loss of HCN

forming the product ion of m/z 39. The two sequential losses of HCN molecules attributed to the pyrimidine structure for the ion of m/z 135 are shown in Figure 4b. In the positive ion EI mass spectra of the unknown compounds, the ions at m/z 137 and 135 were characteristic of the pyrimidine structure, and MS/MS analysis was used to support the proposed ion structures.

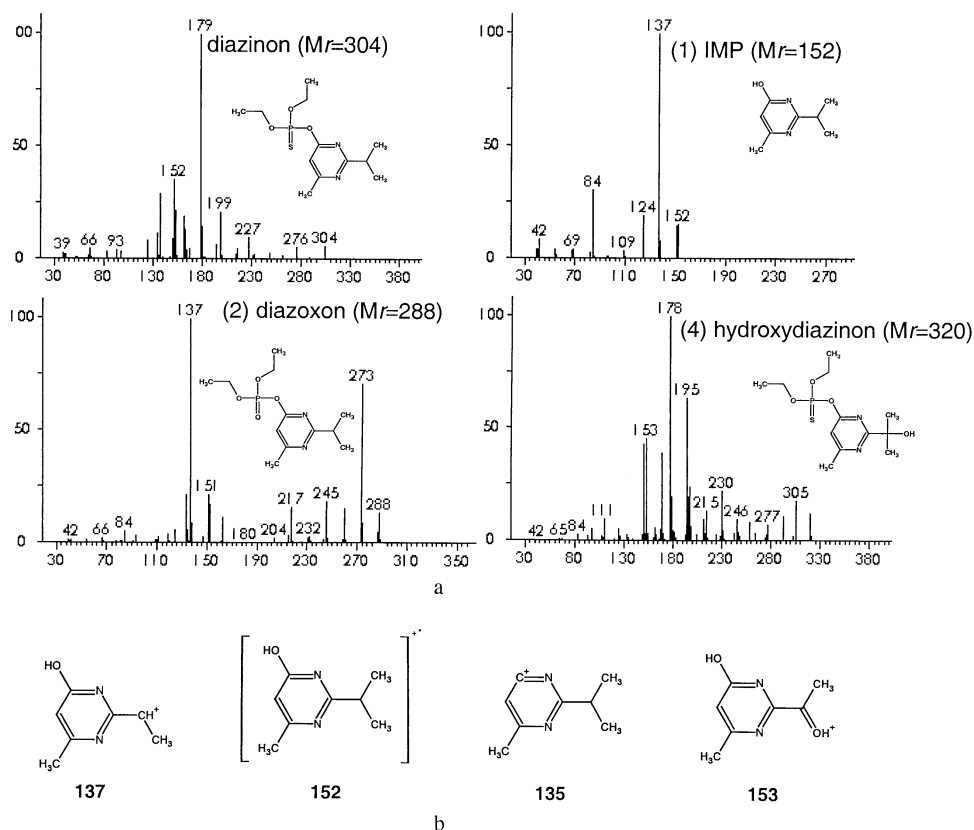The NCI mass spectrum of diazinon showed a base

Figure 4. (**a**) EI mass spectra of diazinon and intermediates identified by comparison with authentic standards (**1**, **2**) or by library searching (**4**), used to confirm the unknown degradation products. (**b**) Proposed structures for fragment ions at m/z 137, 152, 135 and 153.

Table 1. Fragment ions and relative abundances (RA) of diazinon and its degradation products in NCI mode of operation

| Compound	Mr	m/z	Possible structure	RA
Diazinon	304	169	$[C_4H_{10}O_3PS]^-$	100
Diazoxon (**2**)	288	153	$[C_4H_{10}O_4P]^-$	100
		125	$[C_2H_6O_4P]^-$	10
Hydroxydiazinon (**4**)	320	169	$[C_4H_{10}O_3PS]^-$	100
		183	$[C_5H_{14}NO_4P]^{--}$	14
Compound **3a**	304	153	$[C_4H_{10}O_4P]^-$	a
Compound **3b**	318	318	$[C_{12}H_{19}N_2O_4PS]^{--}$	100
		169	$[C_4H_{10}O_3PS]^-$	35
		181	$[C_5H_{12}NO_4P]^{--}$	32
Compound **5**	306	169	$[C_4H_{10}O_3PS]^-$, $[C_4H_{12}NO_4P]^{--}$	100
Compound **6**	304	169	$[C_4H_{10}O_3PS]^-$	100
		167	$[C_4H_{10}NO_4P]^{--}$	27
		304	$[C_{11}H_{17}N_2O_4PS]^{--}$	26
Compound **7**	320	169	$[C_4H_{10}O_3PS]^-$	100
		183	$[C_5H_{14}NO_4P]^{--}$	6

^{a}RA for this fragment ion was not possible to obtain, because of the intereference from coelluted peak **3b**.

peak at m/z 169 (Table 1). The structure of the thiophosphoric moiety of this ion, reported also in a previous study [27], could be well defined using MS^3 for product ions of m/z 141 and m/z 95 (Scheme 1). The ion of m/z 169 provided strong evidence for the presence of the thiophosphoric moiety of diazinon in the organic intermediate structures.

Impurities (**1**) and (**2**) were already present in the diazinon commercial standard used in the photocatalysis experiments. Impurity (**1**) eluted from the GC with a retention time of 23.8 min and was identified as sulfotep (O,O,O,O-tetraethyl dithiodiphosphate) (Mr 322) by comparison with the authentic standard. Impu-

rity (**2**) (RT 29.8 min), molecular mass of 302, formed a fragment ion of m/z 135 that corresponded to the pyrimidine moiety of diazinon based on the MS/MS fragment ions of m/z 93, 66, and 39 (see Figure 4b). The NCI mass spectrum of this degradation product showed only one peak at m/z 167, and the absence of the ion at m/z 169 characteristic of the thiophosphoric moiety of diazinon. Both impurities decomposed completely during the photocatalytic process.

Compounds (**1**) and (**2**), which were detected at retention times of 19.0 and 25.8 min respectively, were identified by comparison with authentic standards as 2-isopropyl-6-methylpyrimidin-4-ol (IMP) and diaz-
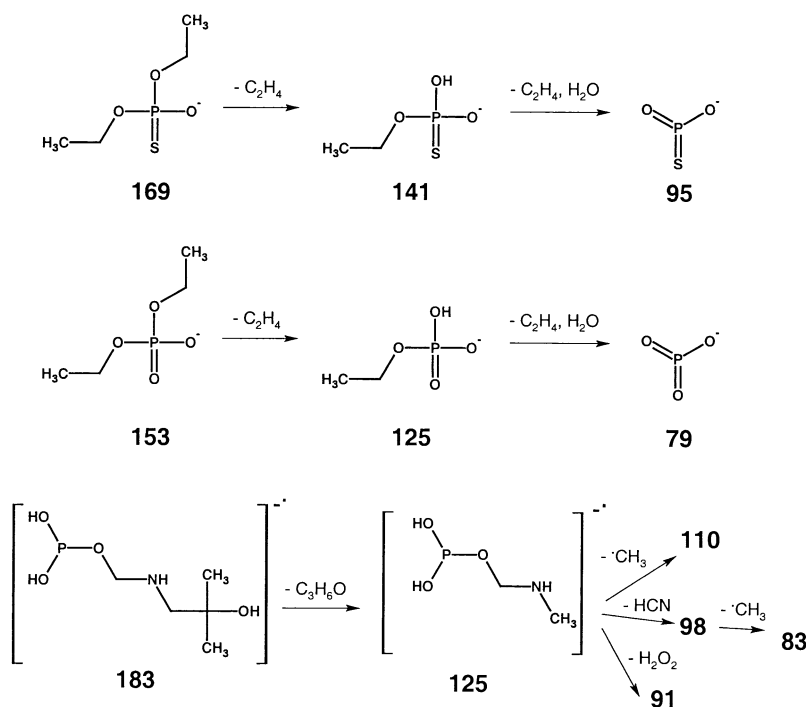
Scheme 1. Fragmentation scheme obtained from MS/MS NCI spectra for species having m/z 169, 153, and 183.
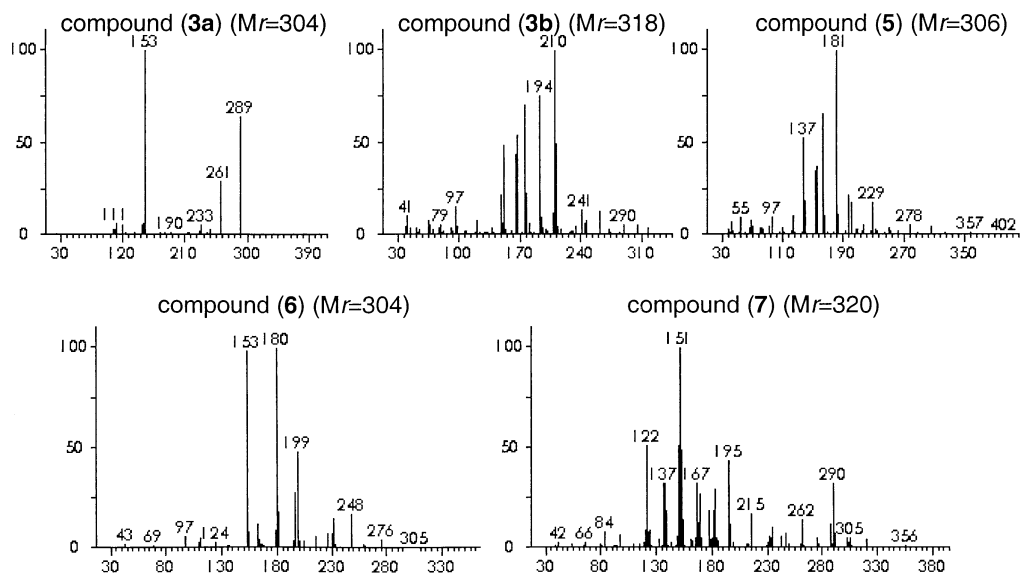
Figure 5. EI mass spectra of compounds identified by mass spectra interpretation. Compounds (**3a**), (**6**), (**7**) were also confirmed by LC/MS.

oxon, each. The base peak at m/z 137 in the mass spectrum of IMP (Figure 4) corresponded to the pyrimidine species produced following the loss of a methyl radical from the molecular ion of m/z 152. The MS/MS fragmentation pattern of the IMP ion of m/z 137 contained the product ion of m/z 84 and was identical to the corresponding MS/MS fragmentation pattern for diazinon. IMP is the hydrolysis product of diazinon formed through the cleavage of P=O(pyrimidine group) bond, that has been found in water, soil, plants, and animals [9, 29]. Diazoxon (Mr 288), the oxygen analogue of diazinon in which S has been replaced by an O atom, has been reported to be a diazinon photolysis product in water/soil suspensions [9] and is a diazinon metabolite formed in vitro and in vivo in studies with animals [30]. The base peak at m/z 137 in the positive ion EI mass spectrum (Figure 4a) of diazoxon is similar to that of diazinon and IMP, but the fragment ion corresponding to the ethyl ether of the pyrimidine group (m/z 179) was not observed. The NCI mass spectrum of diazoxon (Table 1) showed a fragment ion at m/z 153, which is characteristic of a phosphoric moiety and confirmed by MS/MS analysis. Irradiation of diazoxon in TiO_2 aqueous suspensions gave IMP as the main product.

The peak eluting at 27.9 min [Compound (**4**)] during GC/MS was identified as hydroxydiazinon (O,O-diethyl O-[2-(1-hydroxy-1-methylethyl)-6-methylpyrimidin-4-yl] thiophosphate) with a probability higher than 97% by searching the mass spectra library. The positive ion EI mass spectrum of Compound (**4**) in Figure 4a shows several similarities with that of diazinon except for the loss of a H_2O molecule indicating the presence of an alcohol group. Loss of a methyl radical from the molecular ion of m/z 320 formed the ion of m/z 305, which after elimination of C_2H_4 produced the ion at m/z 277. MS/MS fragmentation of the ion of m/z 277 shows

loss of a thiophosphonic moiety ($POSOC_2H_5$, 124 u) giving an ion at m/z 153. Since the ratio of the abundances of the ions of m/z 155:153 in the positive ion EI mass spectrum is ~1%, there is probably no S atom in the ion at m/z 153. Therefore, the proposed molecular structure for the ion at m/z 153 is analogous to the structure of the ion at m/z 152 of diazinon (Figure 4b).

In the NCI mass spectrum of hydroxydiazinon (Table 1) the base peak was detected at m/z 169 which is characteristic of the diazinon thiophosphoric moiety. Another abundant ion was observed at m/z 183, and MS/MS product ion analysis of this ion showed elimination of a neutral molecule of 58 u corresponding to an acetone. MS/MS product ion analysis of the fragment ion of m/z 125 produced loss of a methyl radical, elimination of a molecule of HCN followed by loss of a methyl radical, and a loss of 34 u corresponding to H_2O_2. The structure of the ion at m/z 183 and its fragmentation pathway are shown in Scheme **1**. The introduction of the additional oxygen atom into the isopropyl group played an essential role in the production of this electronegative ion.

Characteristic anions formed during NCI of the degradation products of diazinon were the ions of m/z 169 corresponding to $[(C_2H_5O)_2POS]^-$ of diazinon derivatives, m/z 153 corresponding to $[(C_2H_5O)_2PO_2]^-$ of diazoxon derivatives, and m/z 183, $[P(OH)_2OCH_2NHCH_3(C_3H_7O)]^-$, for hydroxylated diazinon derivatives (Table 1). MS^n was used to support the proposed structures of these ions.

Looking closely at the GC/MS data, a peak (**3**) of low intensity was detected at a retention time of 27.5 min in the GC/MS chromatogram in Figure 3. After detailed examination, this peak was found to contain two overlapping peaks. The positive ion EI mass spectrum of the first peak (**3a**) was characterized by a base peak of m/z
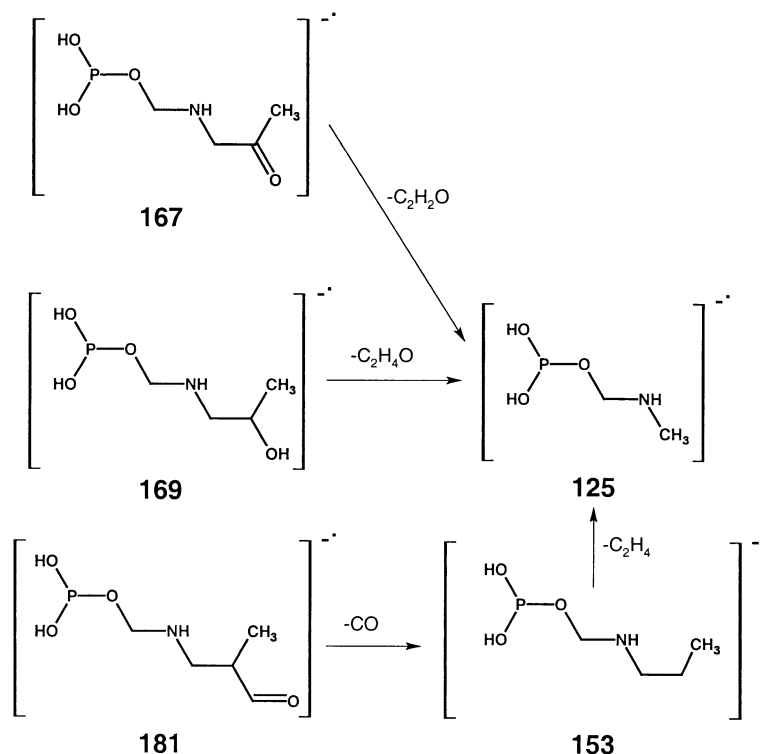
Scheme 2. Fragmentation scheme obtained from MS/MS NCI spectra for species having m/z 167, 169, and 181.

153 (Figure 5), which interestingly produced a fragmentation pattern during MS/MS that was identical to that of hydroxydiazinon. The positive ion CI mass spectrum suggested that the compound had a molecular mass of 304 u, although the signal-to-noise ratio was too low. The NCI mass spectrum of Compound (**3a**) produced an ion of m/z 153 (Table 1), which the MS/MS fragmentation pattern is characteristic of the phosphoric moiety of diazoxon. According to these data, diethyl 2-(1-hydroxy-1-methylethyl)-6-methylpyrimidin-4-yl phosphate (hydroxydiazoxon) is the predominant candidate structure for Compound (**3a**).

The positive ion EI mass spectrum of the second peak (**3b**) eluting at 27.5 min is shown in Figure 5. The low intensity of this peak did not permit subsequent MS/MS analysis. The molecular mass was determined from the EI mass spectrum to be 318 u which was confirmed by the observation of an $[M + H]^+$ ion of 319 using positive ion CI mass spectrometry. An ion of m/z 169, which is characteristic of the thiophosphoric moiety of diazinon, was detected in the NCI mass spectrum (Table 1). MS/MS analysis of the peak of m/z 181 in the NCI mass spectrum exhibited a loss of 28 u corresponding to the loss of CO. MS^3 of the resulting fragment produced fragment ions including one of m/z 125 (Scheme 2). These data suggest the structure of an aldehyde, O,O-diethyl O-[6-methyl-2-(1-methyl-2-oxo-ethyl)pyrimidin-4-yl] thiophosphate for Compound (**3b**).

The positive ion EI mass spectrum of Compound (**5**), which eluted at 28.1 min (see the chromatogram in Figure 3), is shown in Figure 5. The base peak of Compound (**5**) was observed at m/z 181, and the molecular ion was detected at m/z 306. No abundant sample ions were detected using positive ion CI. However, during NCI a base peak was observed at m/z 169 (see Table 1), and MS/MS analysis of this ion produced a fragmentation pattern consistent with a diazinon thiophosphoric moiety and an ion of m/z 125. The product ion of m/z 125 indicates the presence of an additional moiety of m/z 169 besides the thiophosphoric moiety. The fragment ion of m/z 125 was formed from m/z 169 through elimination of C_2H_4O (Scheme 2). MS/MS analysis of m/z 125 did not produce a useful spectrum due to low signal strength. Based on these data, the structure of Compound (**5**) is consistent with the hydroxyethyl derivative of diazinon, O,O-diethyl O-[2-(1-hydroxyethyl)-6-methylpyrimidin-4-yl] thiphosphate, which has been reported to be a diazinon metabolite in animals formed from hydroxydiazinon through dehydration, oxidation and decarboxylation [30].

Compound (**6**) eluting at 28.6 min weighed 304 u, which was identical to that of diazinon. The EI mass spectrum (see Figure 5) showed an intense peak of m/z 153 indicative of a pyrimidine moiety, fragment ions corresponding to $[M -28^{+·}]$, $[M - 56]^+$, typical losses of one and two C_2H_4 groups. The EI MS/MS analysis of the ion of m/z 153 produced a fragment ions similar to those of hydroxydiazinon (Figure 6a). The NCI mass spectrum of Compound (**6**) was considerably different
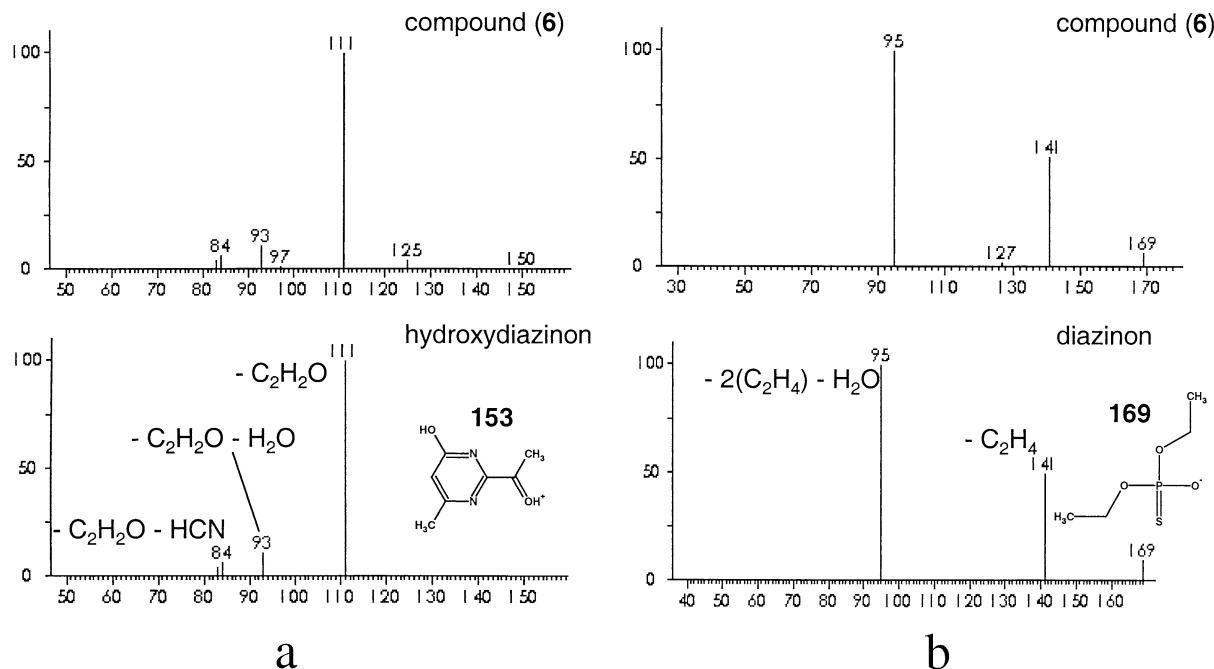
Figure 6. (a) Product-ion EI spectra (GC/MS/MS) of ions at *m/z* 153 of Compound (**6**) (top) and hydroxydiazinon (bottom). (b) Product-ion NCI spectra (GC/MS/MS) of ions at *m/z* 169 of Compound (**6**) (top) and diazinon (bottom).

from that of diazinon and hydroxydiazinon, except for the common ion of *m/z* 169 (Table 1). Under NCI conditions the most abundant fragment ion of *m/z* 169 gave the same MS^3 pattern as the ion of *m/z* 169 of diazinon (Figure 6b). Furthermore, MS/MS analysis of the fragment 167 in the NCI spectrum of this compound showed loss of 42 u (C_2H_2O) giving the ion of *m/z* 125, which MS^3 analysis clearly showed was similar to that ion of hydroxydiazinon (Schemes 1,2). Based on the loss of C_2H_2O, the structure of an acetyl group was indicated for the ion of *m/z* 167. These data suggest that Compound (**6**) is O-(2-acetyl-6-methylpyrimidin-4-yl) O,O-diethyl thiophosphate (diazinon methyl ketone).

Compound (**7**) eluted at 29.3 min in the GC/MS chromatogram shown in Figure 3, and the positive ion EI mass spectrum (see Figure 5) indicated that it had a molecular mass of 320. Fragment ions were observed at [M − 17]$^+$ and [M − 30]$^{+\cdot}$ corresponding to the loss of OH$^-$ and HCHO, respectively. These fragment ions suggest the presence of a free hydroxyl group linked to a primary carbon atom. The ion of *m/z* 137 in the EI mass spectrum of Compound (**7**) was probably formed from the pyrimidine group since its MS/MS spectrum contained ions such as *m/z* 84 like that in the IMP MS/MS spectrum of the ion of *m/z* 137 (Figure 4). The base peak at *m/z* 151 corresponded to the loss of the thiophosphoric moiety from the molecular ion. The fragmentation pattern observed in the NCI mass spectrum of Compound (**7**) supported the presence of the thiophosphoric moiety, since the fragment ion of *m/z* 169 was the base peak (Table 1). Additional confirmation of the presence of a hydroxyl group linked to a

primary carbon atom was obtained using NCI MS/MS of the ion at *m/z* 183. Elimination of a neutral weighing 30 u corresponding to a formaldehyde molecule was observed instead of the loss of an acetone molecule as in the case of hydroxydiazinon (Scheme 1). There are two possibilities for the position of the hydroxyl group, either on the aromatic methyl group resulting hydroxymethyl diazinon or on the methyl group in the isopropyl moiety giving 2-hydroxydiazinon. In metabolism studies carried out in sheep, hydroxymethyl diazinon was identified using NMR, IR and mass spectrometry [31]. The positive ion EI mass spectrum of hydroxymethyl diazinon provided in this paper contained a base peak at *m/z* 195 but no ion of *m/z* 137, which was different from the EI mass spectrum of Compound (**7**) (base peak at *m/z* 151). Based on this evidence, Compound (**7**) is tentatively identified as 2-hydroxydiazinon (O,O-diethyl-O-[2-(2-hydroxy-1-methylethyl)-6-methylpyrimidin-4-yl] thiophosphate).

Compounds (**8**) and (**9**) eluting during GC/MS at 30.8 and 31.7 min, respectively, were probably photoproducts of impurity (**2**) of the diazinon standard used in the irradiation experiments. Their molecular masses, confirmed by positive ion CI mass spectrometry, were 318 u and 302 u, respectively. On the basis of positive ion EI and NCI mass spectrometric analyses, Compound (**8**) was attributed to the 1-hydroxy derivative of impurity (**2**) while Compound (**9**) was tentatively identified as an acetyl derivative of impurity (**2**).

LC/MS. In order to determine elemental compositions, selected extracts of the irradiated aqueous suspensions
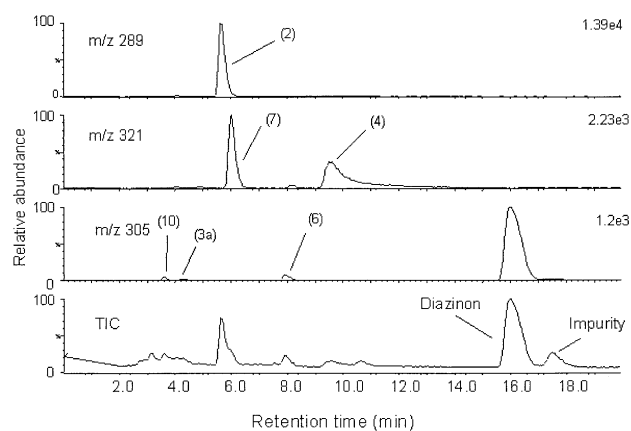
Figure 7. LC-MS chromatograms of a diazinon suspension irradiated for 3 min. The numbers (**2**), (**3a**), (**4**), (**6**), (**7**) correspond to compounds identified also by GC/MS.

were analyzed by LC/MS with positive ion electrospray ionization, and exact mass measurements of the protonated molecules were obtained on-line using a

QqTOF mass spectrometer. In addition, exact mass measurements of the product ions of these species obtained during LC/MS/MS provided valuable information regarding their structures. LC/MS facilitated the detection of several compounds, five of which were detected also using GC/MS. Figure 7 shows the LC/MS chromatogram of a concentrated extract of an aqueous diazinon TiO_2 suspension after 3 min of irradiation. Peaks eluting at retention times of 5.7 and 16.0 min were identified as diazoxon and diazinon, respectively, after comparison with the retention times and fragmentation patterns of authentic standards.

Exact mass measurements and elemental compositions of diazinon, its degradation products and their fragment ions are presented in Table 2. The product ion mass spectra of diazinon and diazoxon were examined to obtain useful information for the interpretation of the product ion spectra of the unknown degradation products. The positive ion electrospray MS/MS spectrum of diazinon is shown in Figure 8b. The two most abundant fragment ions were detected at m/z 169 and 153, and the

Table 2. Exact mass measurements and elemental composition of diazinon, its degradation products and their fragment ions using LC/MS/MS analysis

Compound	Observed mass ([M + H]$^+$)	Major ions (relative abundance)	Calculated mass	Elemental composition	Error (ppm)
Diazinon	305.100	305.1100 (100)	305.1089	$C_{12}H_{22}N_2O_3PS$	+3.7
		169.0810 (50)	169.0799	$C_8H_{13}N_2S$	+6.2
		153.1032 (30)	153.1028	$C_8H_{13}N_2O$	+2.7
Diazoxon (**2**)	289.1317	289.1317 (100)	289.1317	$C_{12}H_{22}N_2O_4P$	0.0
		153.1030 (97)	153.1028	$C_8H_{13}N_2O$	+1.4
2-Hydroxydiazinon (**7**)	321.1043	321.1043 (100)	321.1038	$C_{12}H_{22}N_2O_4PS$	+1.6
		185.0749 (72)	185.0749	$C_8H_{13}N_2OS$	+0.0
		293.0710 (10)	293.0725	$C_{10}H_{18}N_2O_3PS$	−9.4
		169.0957 (8)	169.0977	$C_8H_{13}N_2O_2$	−11.8
		155.0891 (2)	155.0821	$C_7H_{11}N_2O_2$	+45.4
Hydroxydiazinon (**4**)	321.1048	321.1048 (29)	321.1038	$C_{12}H_{22}N_2O_3PS$	+3.1
		303.0942 (100)	303.0932	$C_{12}H_{20}N_2O_3PS$	+3.5
		247.0321 (13)	247.0306	$C_8H_{12}N_2O_3PS$	+6.0
		167.0642 (6)	167.0643	$C_8H_{11}N_2S$	−0.6
		151.0881 (6)	151.0871	$C_8H_{11}N_2O$	+6.4
2-Hydroxydiazoxon (**10**)	305.1271	305.1271 (100)	305.1266	$C_{12}H_{22}N_2O_5P$	+1.5
		277.0982 (10)	277.0953	$C_{10}H_{18}N_2O_5P$	+10.4
		275.1184 (11)	275.1161	$C_{11}H_{20}N_2O_4P$	+8.5
		249.0667 (7)	249.0640	$C_8H_{14}N_2O_5P$	+10.7
		169.0987 (77)	169.0977	$C_8H_{13}N_2O_2$	+5.9
Hydroxydiazoxon (**3a**)	305.1264	305.1264 (20)	305.1266	$C_{12}H_{22}N_2O_5P$	−0.7
		287.1182 (100)	287.1161	$C_{12}H_{20}N_2O_4P$	+7.4
		259.0870 (20)	259.0848	$C_{10}H_{16}N_2O_4P$	+8.6
		231.0551 (10)	231.0535	$C_8H_{12}N_2O_4P$	+7.1
		169.0991 (8)	169.0977	$C_8H_{13}N_2O_2$	+8.3
		151.0858 (10)	151.0871	$C_8H_{11}N_2O$	−8.9
Diazinon methyl ketone (**6**)	305.0729	305.0729 (82)	305.0725	$C_{11}H_{18}N_2O_4PS$	+1.3
		277.0396 (31)	277.0412	$C_9H_{14}N_2O_4PS$	−5.7
		169.0440 (100)	169.0436	$C_7H_9N_2O_2$	+2.6
		153.0665 (57)	153.0664	$C_7H_9N_2O_2$	+0.6
		153.0155 (15)	153.0139	$C_4H_{10}O_2PS$	+10.4
		124.9839 (18)	124.9826	$C_2H_6O_2PS$	+10.3

Note: Exact masses of precursor ions are those obtained using LC/MS. For fragmentation studies centroids were obtained using theoretical formula of precursor ion as the lock mass.
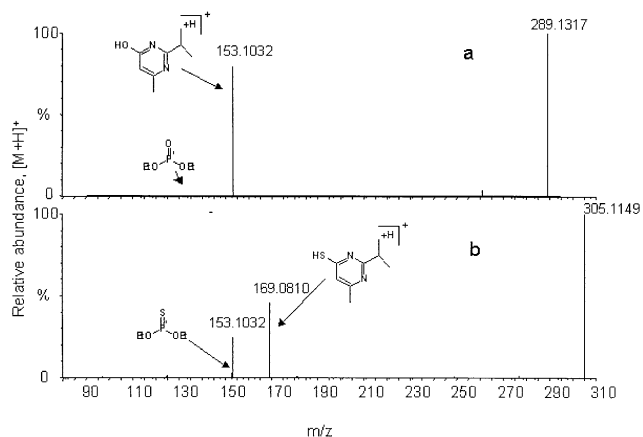
Figure 8. Product ion spectra of (**a**) diazoxon and (**b**) diazinon, at 15eV.

exact masses of these ions were consistent with elemental compositions of $C_8H_{13}N_2S$ and $C_8H_{13}N_2O$, respectively. Close examination of the MS/MS spectrum at m/z 153 revealed the presence of another small, baseline-resolved ion of m/z 153.0155 corresponding to an elemental composition of $C_4H_{10}O_2PS$. Possible mechanisms for the formation of the most abundant fragment ions of diazinon are shown in Scheme 3. Ions at m/z 277 and 249 represent consecutive eliminations of ethylene molecules and were probably formed by a classical

elimination reaction involving a four-member transition state. The abundant fragment ion at m/z 153.1032 might be formed by a similar mechanism involving transfer of hydrogen from the phosphoric OH group. Alternatively, this ion might have been formed via hydrogen transfer through a favorable six-member transition state as depicted in Scheme 3. The product ion of m/z 169.0810 could be formed by the same mechanism after thiono-thiolo rearrangement of the precursor ion. Thiono-thiolo rearrangement is a well-known process that can be either thermally driven or proton catalyzed, and both of which can occur in the mass spectrometer. The formation of the minor ion at m/z 153.0155 might be rationalized by protonation of the oxygen atom followed by inductive cleavage and charge migration.

The positive ion electrospray MS/MS product ion mass spectrum of diazoxon (Figure 8a) showed the same abundant fragment ions as diazinon. For example, the most abundant product ion was detected at m/z 153 with an elemental composition of $C_8H_{13}N_2O$. In addition, an ion corresponding to the phosphoric moiety was detected at m/z 135 indicating that P=S was oxidized to P=O.

Two species having protonated molecules of m/z 321 eluted at retention times of 6.0 and 9.6 min during LC/MS suggesting the formation of mono-oxidation products of diazinon (Figure 7). Based on exact mass
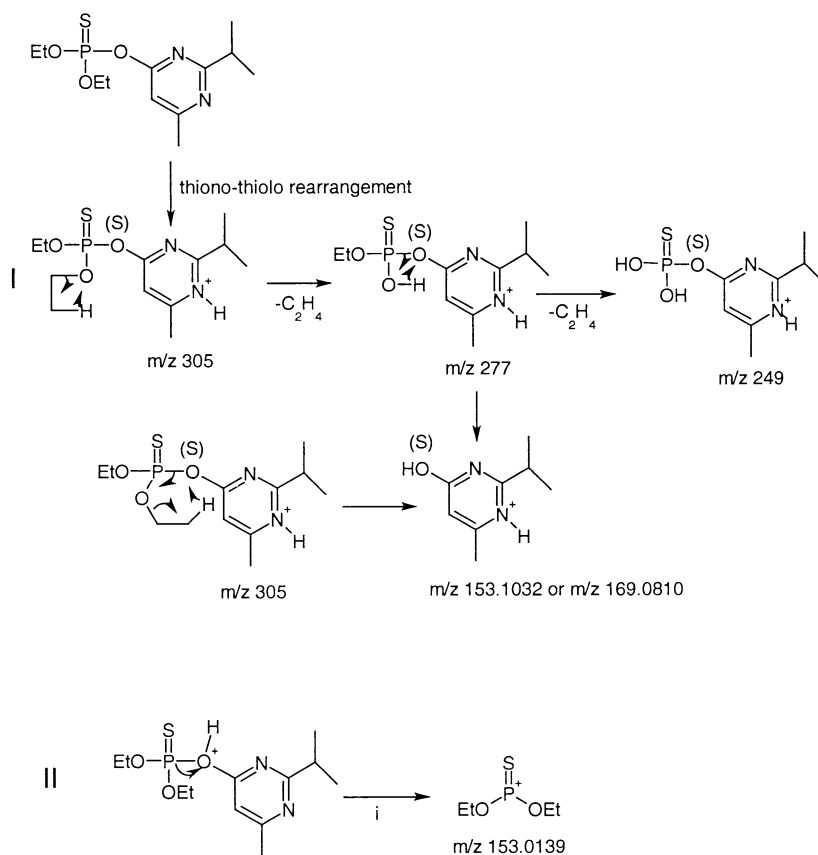
Scheme 3. Proposed fragmentation pathway of diazinon obtained from LC/MS/MS analysis.
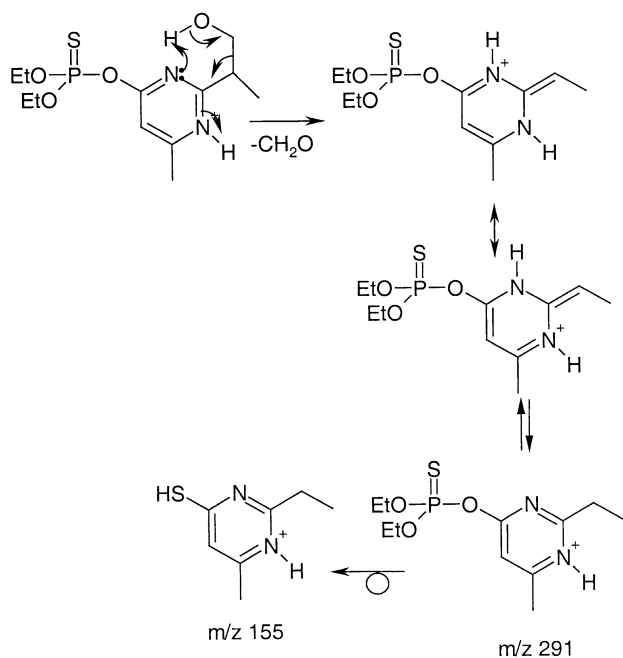
Scheme 4. Proposed fragmentation pathway of 2-hydroxydiazinon obtained from LC/MS/MS analysis.

measurements, the elemental composition for the two compounds was determined to be $C_{12}H_{21}N_2O_4PS$, which confirms oxidation and introduction of one oxygen atom each. Examination of the product ion mass spectra of the two compounds revealed that oxidation took place on the pyrimidine and not on the thiophosphoric moiety. For example, the product ion mass spectrum of the peak eluting at 6.0 min showed an abundant fragment ion at m/z 185 with an elemental composition of $C_8H_{13}N_2OS$. The fragment ion corresponding to the loss of water from the precursor ion was low in abundance suggesting that elimination of water was not a facile process. Furthermore, a diagnostic fragment ion corresponding to the loss of a molecule of formaldehyde was observed at m/z 291. This ion is frequently observed in mass spectra of molecules containing a hydroxymethyl group. There are two possibilities for this structural feature, either hydroxylation of an aromatic methyl group resulting hydroxymethyldiazinon, or oxidation of the methyl group in the isopropyl moiety forming 2-hydroxydiazinon. The structure of this peak probably corresponds to 2-hydroxydiazinon (**7**). Elimination of a formaldehyde molecule from 2-hydroxydiazinon might proceed via a favorable six-member transition state as shown in Scheme **4**. The resulting fragment ion might tautomerize into an aromatic structure. However, formation of such a stable ion is not possible for hydroxymethyldiazinon. It should be noted that 2-hydroxydiazinon was also identified by using GC/MS.

The peak eluting at 9.6 min showed an abundant fragment corresponding to loss of water from the precursor ion. The only other fragmentation pathway included sequential losses of ethylene molecules. The most probable structure for this diazinon degradation product was hydroxydiazinon (**4**), which had also been identified tentatively using GC/MS.

There were several peaks with the same nominal mass as diazinon of m/z 305. The exact masses of these peaks eluting at 3.6 and 4.3 min were determined to be 305.1271 and 305.1264 corresponding to an elemental composition of $C_{12}H_{21}N_2O_5P$. This composition suggests that these peaks represent oxidation products of diazoxon. The identities of these oxidation products were tentatively determined based on the comparison of their MS/MS fragmentation pathways to those of known oxidation products of diazinon. The product ion MS/MS spectrum of the compound with an apparent protonated molecule of m/z 305 eluting at 3.6 min showed an abundant fragment ion of m/z 169 suggesting that oxidation took place on the pyrimidine moiety of the molecule. The relative abundances of the ions of m/z 151 and 287, corresponding to loss of water from the fragment ions of m/z 169 and from the precursor ion of m/z 305, were low. This information and the observation of an ion of m/z 275 corresponding to the loss of a formaldehyde molecule from the protonated molecule support the assignment of this peak as 2-hydroxydiazoxon (**10**).

The most abundant fragment ion in the product ion mass spectrum of the peak eluting at 4.3 min was detected at m/z 287 and corresponded to elimination of water. This suggests that oxidation occurred on the secondary carbon atom of the isopropyl group of diazoxon. By analogy with hydroxydiazinon, this peak was tentatively identified as hydroxydiazoxon (**3a**), which was also detected during GC/MS analysis.

Of particular interest was the peak eluting at 7.9 min. Based on exact mass measurements, the elemental composition of this ion was determined to be $C_{11}H_{17}N_2O_4P$. This elemental composition indicates that the diazinon precursor had lost a methane molecule as well as been mono-oxygenated. In the product ion spectrum, the most abundant fragment ions were detected at m/z 153 and 169. Using exact mass measurements, the elemental compositions of these product ions were determined to be $C_7H_9N_2O_2$ and $C_7H_9N_2OS$, respectively. Together with the presence of small ion of m/z 153.0155, these data clearly show that modifications occurred on the pyrimidine moiety instead of the thiophosphoric part of the molecule. Based on the data above, it appears that oxygen introduced during oxidation was not in the form of a hydroxyl group. Instead, the elemental composition may be rationalized by formation of a ketone with the elimination of methane from the isopropyl substituent on pyrimidine ring. Therefore, Compound (**6**) is probably diazinon methyl ketone which is an intermediate detected also during GC/MS analysis.

The peak eluting at 10.5 min in Figure 7 had a protonated molecule of m/z 337. The exact mass measurement of m/z 337.0987 indicated a molecular composition of $C_{12}H_{21}N_2O_5PS$ showing that two oxygen atoms

had been introduced into diazinon. The LC/MS/MS product ion mass spectrum revealed unusual fragmentation dominated by the loss of methanol (32 u) as well as elimination of hydrogen peroxide (34 u). More definitive structural evaluation was prevented by the low concentration of this compound in the extracted samples. Finally in Figure 7, two peaks with retention times of 7.5 and 17.5 min and protonated molecules of m/z 303 were assigned to diazinon commercial standard impurities or impurity photoproducts.

Degradation Pathway

The formation of diazinon photocatalytic degradation products as a function of the irradiation time was followed by using GC/MS and is shown in Figure 9. However, hydroxydiazoxon [Compound (3a)], which is a double oxidation product of diazinon, showed a delayed maximum level of ~5 min supporting its formation through the intermediate oxidation of diazinon to diazoxon. During these first minutes of irradiation, 70% of the initial concentration of diazinon was converted into Compounds (1–7) while the recovery of CO_2 during this time was negligible. It should be noted that none of these products was detected after 30 min of irradiation. Even though a further oxidation leads to the ring-opening and the formation of aliphatic oxidation derivatives, these species will not be discussed.

Based on the GC/MS and LC/MS analyses of the various photocatalytic intermediates, a degradation pathway for diazinon is proposed in Scheme 5. There are two different major oxidative routes of degradation. One route involves the cleavage of the P–O(pyrimidine group) bond yielding IMP. In the photocatalytic process loss of the pyrimidine group probably occurs either through oxidative desulfuration by OH radical attack [32] on the thiono group to give diazoxon followed by hydrolysis, or through an oxidative mechanism acting directly on diazinon. These oxidative mechanisms have already been observed for most thiophosphates in metabolic studies [33]. In the second route, the thiophosphoric moiety of diazinon is preserved. Hydroxylation of the primary or secondary carbon atoms of the isopropyl group gave hydroxydiazinon (4) or 2-hydroxydiazinon (7), respectively, which after further oxidation led to diazinon aldehyde (3b) and diazinon methyl ketone (6). A similar transformation pathway was observed following for the oxygen analogue diazoxon formed by oxidation of the P=S bond of diazinon to a P=O bond which led to the formation of the hydroxylated derivatives (3a, 10).

Conversion to various hydroxylated metabolites of diazinon has been also observed in metabolism studies with animals. Enzymatic hydroxylation of the isopropyl group was found to be the major transformation pathway *in vivo* and *in vitro* [34]. Although hydroxydiazinon (4) and hydroxydiazoxon (3a) have been reported in various metabolism studies [30, 35], oxidative derivatives of the primary carbon atom of the isopropyl group of diazinon (3b, 7) e.g., 2-hy-
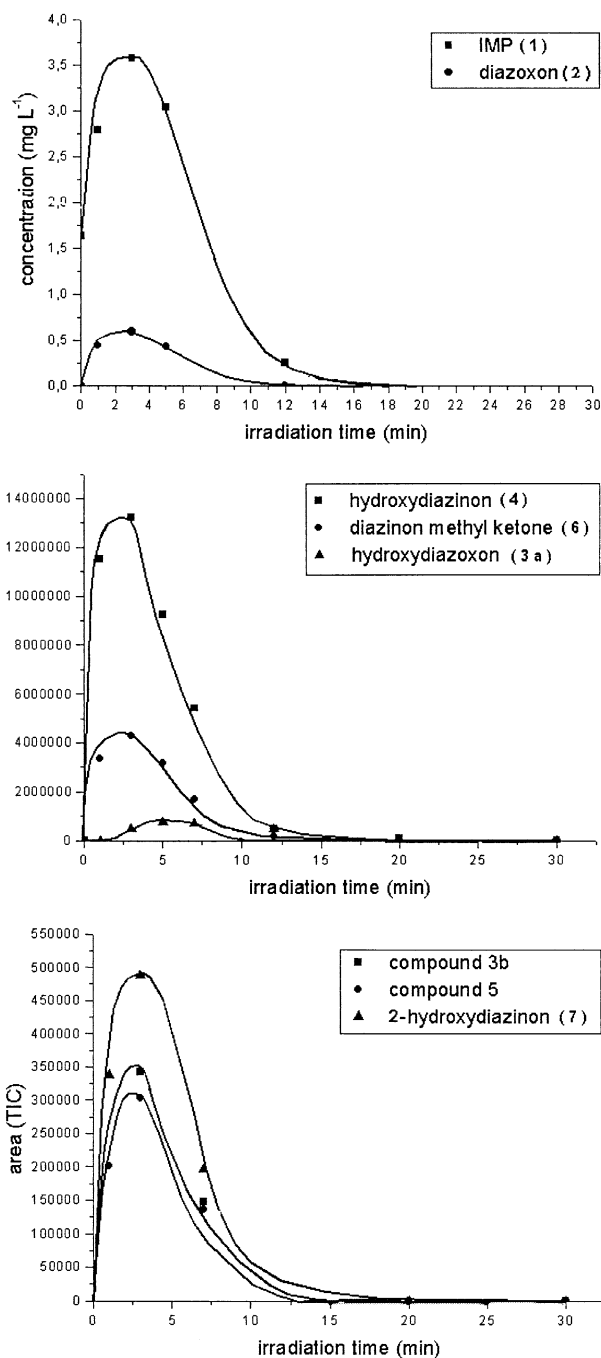

Figure 9. Formation and degradation of diazinon organic intermediates occuring during TiO_2 induced photocatalysis.

droxy metabolites, were not observed. In a study of tissue metabolism [30] hydroxydiazinon (4) was reported to occur through a dehydration reaction of the 1-hydroxy-isopropyl group to form an isopropenyl substituted compound which was further oxidized and decarboxylated to the hydroxyethyl derivative (5).

Conclusions

The photocatalytic degradation of diazinon catalyzed by titanium dioxide was observed to proceed essen-
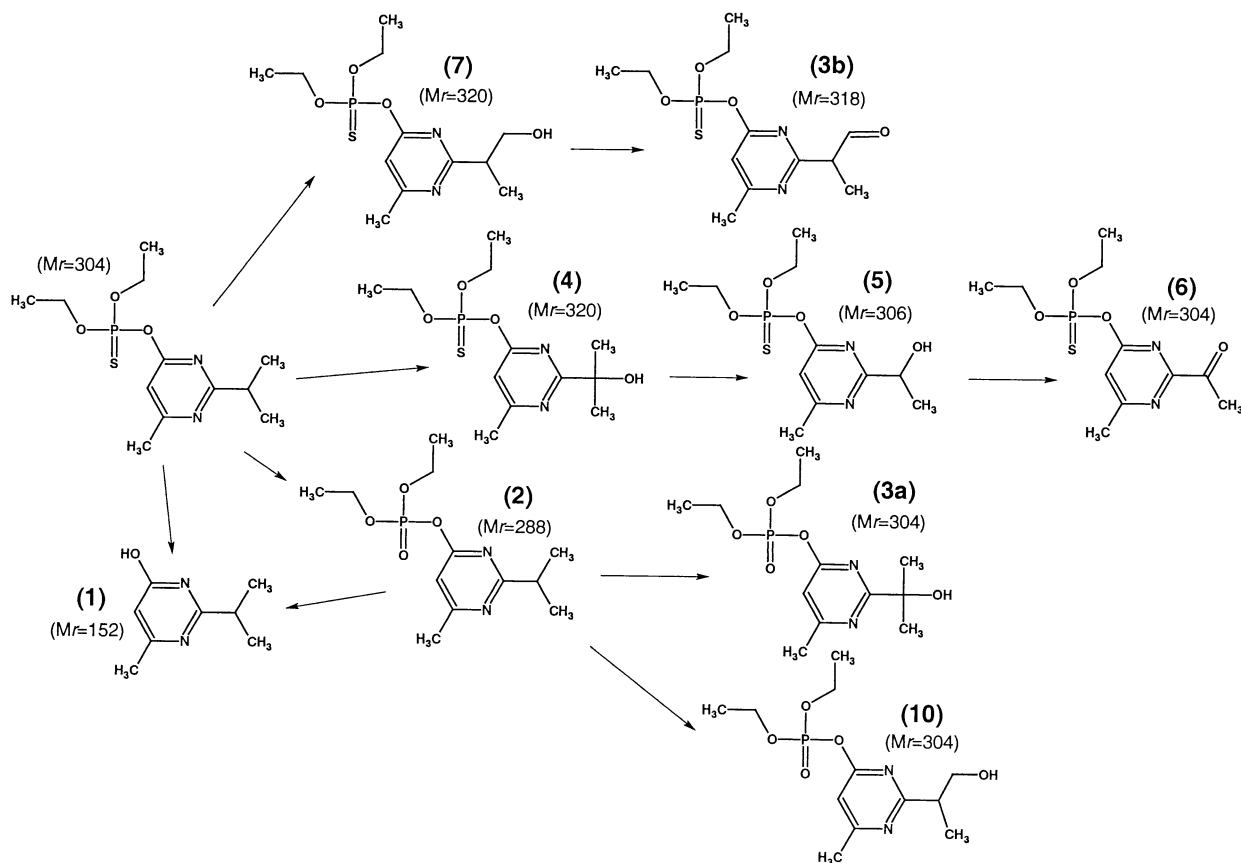
Scheme 5. Scheme of the proposed degradation pathways for diazinon TiO$_2$ induced photocatalysis: IMP (**1**), diazoxon (**2**), hydroxydiazoxon (**3a**), diazinon aldehyde (**3b**), hydroxydiazinon (**4**), hydroxyethyl derivative of diazinon (**5**), diazinon methyl ketone (**6**), 2-hydroxydiazinon (**7**), 2-hydroxydiazoxon (**10**).

tially through a hydroxylation mechanism occurring rapidly by attack of the photocatalytically generated OH radicals. The main transformation intermediates identified were oxidation products of the isopropyl group of diazinon and its oxygen analogue diazoxon. Loss of the thiophosphoric moiety yielded the pyrimidinol IMP.

The results reported here show that the combination of GC/MS/MS with EI, positive and negative ion CI, and LC/MS/MS with electrospray ionization and exact mass measurements represent a powerful analytical approach for the confirmation of the molecular structure of photocatalytic intermediates. The formation of identical diazinon derivatives in metabolism studies may be explained by similar oxidation mechanisms or energetically preferable oxidation pathways.

References

1. Dubus, I.; Hollis, J.; Brown, C. Pesticides in Rainfall in Europe. *Env. Pollut.* **2000,** *110,* 331–344.
2. Garcia, S.; Ake, C.; Clement, B.; Huebuer, H.; Donnelly, K.; Shalat, S. Initial Results of Environmental Monitoring in the Texas Rio Grande Valley. *Environ. Int.* **2001,** *26,* 465–474.
3. Albanis, T.; Hela, D.; Sakellarides, T.; Konstantinou, I. Monitoring of Pesticide Residues and Their Metabolites in Surface and Underground Waters of Imathia (N. Greece) by Means of Solid-Phase Extraction Disks and Gas Chromatography. *J. Chrom. A* **1998,** *823,* 59–71.
4. Bailey, H.; Deanovic, L.; Reyes, E.; Kimball, T.; Larson, K.; Cortright, K.; Connor, V.; Hinton, D. Diazinon and Chlorpyrifos in Urban Waterways in Northern California, USA. *Environ. Toxicol. Chem.* **2000,** *19,* 82–87.
5. Bailey, H.; Kraddoi, R.; Elphick, J.; Mulhall, A.; Hunt, P.; Tedmanson, L.; Lovell, A. Whole Effluent Toxicity of Sewage Treatment Plants in the Hawkesbury-Nepean Watershed, New South Wales, Australia, to Ceriodaphnia dubis and Selenastrum capricornutum. *Environ. Toxicol. Chem.* **2000,** *19,* 72–81.
6. Roberts, T.; Hutson, D., Eds. in Chief.; *Metabolic Pathways of Agrochemicals—Part 2: Insecticides and Fungicides*; RSC: UK, 1999, pp 258–263.
7. Diazinon cancellation order 4/01, EPA2001.
8. Ku, Y.; Chang, J. Effect of Solution pH on the Hydrolysis and Photolysis of Diazinon in Aqueous Solution. *Water Air Soil Pollut.* **1998,** *108,* 445–456.
9. Mansour, M.; Feicht, E.; Behechti, A.; Schramm, K.-W.; Kettrup, A. Determination Photostability of Selected Agrochemicals in Water and Soil. *Chemosphere* **1999,** *39,* 575–585.
10. Scheunert, I.; Mansour, M.; Dorfler, U.; Schroll, R. Fate of Pendimethalin, Carbofuran, and Diazinon under Abiotic and Biotic Conditions. *Science Total Environ.* **1993,** *132,* 361–369.
11. Lacorte, S.; Lartiges, S.; Garrigues, P.; Barcelo, D. Degradation of Organophosphorus Pesticides and Their Transformation

Products in Estuarine Waters. *Environ. Sci. Technol.* **1995,** *29,* 431–438.

12. Mills, A. Le; Hunte, S. An Overview of Semiconductor Photocatalysis. *J. Photochem. Photobiol. A. Chem.* **1997,** *108,* 1–35.

13. Fujishima, A.; Rao, T.; Tryk, D. Titanium Dioxide Photocatalysis. *J. Photochem. Photobiol. A. Chem.* **2000,** *1,* 1–21.

14. Muszkat, L.; Bir, L.; Feigelson, L. Solar Photocatalytic Mineralization of Pesticides in Polluted Waters. *J. Photochem. Photobiol. A. Chem.* **1995,** *87,* 85–88.

15. Guillard, C.; Pichat, P.; Huber, G.; Hoang-Van, C. The GC-MS Analysis of Organic Intermediates from the TiO$_2$ Photocatalytic Treatment of Water Contaminated by Lindane (1α,2α,3β,4α,5α,6β-hexachlorocyclohexane). *J. Adv. Oxid. Technol.* **1996,** *1,* 53–60.

16. Topalov, A.; Molnar-Gabor, D.; Kosanic, M.; Abramovic, B. Photomineralization of the Herbicide Mecoprop Dissolved in Water Sensitized by TiO$_2$. *Water Res.* **2000,** *34,* 1473–1478.

17. Herrmann, J-M.; Guillard, C.; Arguello, M.; Aguera, A.; Tejedor, A.; Piedra, L.; Fernandez-Alba, A. Photocatalytic Degradation of Pesticide Pirimiphos-Methyl. Determination of the Reaction Pathway and Identification of Intermediate Products by Various Analytical Methods. *Catal. Today* **1999,** *54,* 353–367.

18. Hiskia, A.; Mylonas, A.; Papaconstantinou, E. Comparison of the Photoredox Properties of Polyoxometallates and Semiconducting Particles. *Chem. Soc. Rev.* **2001,** *30,* 62–69.

19. Mak, M.; Hung, S. Degradation of Neat and Commercial Samples of Organophosphate Pesticides in Illuminated TiO$_2$ Suspensions. *Toxicol. Environ. Chem.* **1992,** *36,* 155–168.

20. Mas, D.; Hisanaga, T.; Pichat, P. Photoatalytic Degradation of the Pesticides Asulam and Diazinon in TiO2 Aqueous Suspensions. *Trends Photochem. Photobiol.* **1994,** *3,* 467–479.

21. Meijers, R.; Oderwaldmuller, E.; Nuhn, P.; Kruithof, J. Degradation of Pesticides by Ozonation and Advanced Oxidation. *Ozone-Sci. Eng.* **1995,** *17,* 673–686.

22. Doong, R.; Chang, W. Photoassisted Titanium Dioxide Mediated Degradation of Organophosphorus Pesticides by Hydrogen Peroxide. *J. Photochem. Photobiol. A. Chem.* **1997,** *107,* 239–244.

23. Hasegawa, K.; Kanbara, T.; Kagaya, S. Photocatalyzed Degradation of Agrochemicals in TiO$_2$ Aqueous Suspensions. *Denki Kagaku* **1998,** *66,* 625–634.

24. San, N.; Hatipoglu, A.; Kocturk, G.; Cinar, Z. Photocatalytic Degradation of 4-Nitrophenol in Aqueous TiO$_2$ Suspensions: Theoritical Prediction of the Intermediates. *J. Photochem. Photobiol. A. Chem.* **2002,** *146,* 189–197.

25. Calza, P.; Pelizzetti, E.; Brussino, M.; Baiocchi, C. Ion Trap Tandem Mass Spectrometry Study of Dexamethasone Transformation Products on Light Activated TiO$_2$ Surface. *J. Am. Soc. Mass Spectrom.* **2001,** *12,* 1286–1295.

26. D'Oliveira, J.; Minero, C.; Pelizzetti, E.; Pichat, P. Photodegradation of Dichlorophenols and Trichlorophenols in TiO$_2$ Aqueous Suspensions: Kinetic Effects of the Positions of the Cl Atoms and Identification of the Intermediates. *J. Photochem. Photobiol. A* **1993,** *72,* 261–267.

27. Stan, H.; Kellner, G. Negative Chemical Ionization Mass Spectrometry of Organophosphorus Pesticides. *Biomed. Mass Spectrom.* **1982,** *9,* 483–492.

28. Lopez-Avila, V. Mass Spectral Fragmentation of Diazinon and Diazinon-*d*10 under Electron Impact. *Org. Mass Spectrom.* **1985,** *20,* 530–532.

29. Mucke, W.; Alt, K.; Esser, H. Degradation of 14C-Labeled Diazinon in the Rat. *J. Agri. Food Chem.* **1970,** *18,* 208–212.

30. Miyazaki, H.; Tojinbara, I.; Watanabe, Y.; Osaka, T.; Okui, S. Studies on Metabolism of Diazinon [O,O-Diethyl-O-(2-Isopropyl-4-Methyl-6-Pyrimidinyl)Phosphorothioate] in Animals and Plants. *Proceedings of the First Symposium on Drug Metabolism Action*; Chiba, Japan, 1970; pp 135–138.

31. Janes, N.; Machin, A.; Quick, M.; Rogers, H.; Mundy, D.; Cross, A. Toxic Metabolites of Diazinon in Sheep. *J. Agri. Food Chem.* **1973,** *21,* 121–124.

32. Atkinson, R.; Aschmann, S.; Arey, J.; McElroy, P.; Winer, A. Product Formation from the Gas-Phase Reactions of the OH Radical with (CH$_3$O)PS and (CH$_3$O)$_2$P(S)SCH$_3$. *Environ. Sci. Technol.* **1989,** *23,* 243–244.

33. Yang, R.; Hodgson, E.; Dauterman, W. Metabolism in Vitro of Diazinon and Diazoxon in Rat Liver. *J. Agri. Food Chem.* **1971,** *19,* 10–13.

34. Machin, A.; Rogers, H.; Cross, A.; Quick, M.; Howells, L.; Janes, N. Metabolic Aspects of the Toxicology of Diazinon I. Hepatic Metabolism in the Sheep, Cow, Pig, Guinea-Pig, Rat, Turkey, Chicken, and Duck. *Pesticide Sci.* **1975,** *6,* 461–473.

35. Shishido, T.; Fukami, J. Enzymatic Conjugation of Diazinon with Glutathione in Rat and American Cockroach. *Pesticide Biochem. Physiol.* **1972,** *2,* 39–50.